Open Journal of Yangtze Gas and Oil, 2024, 9, 1-31
https://www.scirp.org/journal/ojogas
ISSN Online: 2473-1900
ISSN Print: 2473-1889

Evaluation and Optimization of the Production System of the Mibale Field: Case of the MIB-14ST2 Well in the Offshore of the Coastal Basin of the Democratic Republic of the Congo

Joel Kabesa Kilungu[1], Bavon Diemu Tshiband[1], Dona Kampata Mbwelele[1], Joseph Lukola Empenga[1], Dominique Wetshondo Osomba[2]

[1]Department of Exploration-Production, Faculty of Oil, Gas and Renew Energies, University of Kinshasa, Kinshasa, Democratic Republic of the Congo
[2]Department of Geosciences, Faculty of Science, University of Kinshasa, Kinshasa, Democratic Republic of the Congo
Email: joel.kabesa@unikin.ac.cd, angediemu@hotmail.com, dona.kampata@gmail.com, josephempenga@gmail.com, dwosomba2012@yahoo.fr

How to cite this paper: Kilungu, J.K., Tshiband, B.D., Mbwelele, D.K., Empenga, J.L. and Osomba, D.W. (2024) Evaluation and Optimization of the Production System of the Mibale Field: Case of the MIB-14ST2 Well in the Offshore of the Coastal Basin of the Democratic Republic of the Congo. *Open Journal of Yangtze Gas and Oil*, **9**, 1-31.
https://doi.org/10.4236/ojogas.2024.91001

Received: January 5, 2024
Accepted: January 28, 2024
Published: January 31, 2024

Abstract

Optimizing the hydrocarbon production system is a fundamental practice to ensure the recovery of developed reserves while maximizing the yield of the oil field. Therefore, several methods and techniques are used to optimize a production system, but the one used in the Mibale field is nodal analysis because it allows for easy understanding of a production system by quickly identifying the problem in order to find optimal solutions. Located in the offshore coastal basin of the Democratic Republic of the Congo and discovered in 1973, the Mibale field has begun to produce an initial flow rate of 10,000 BOPD since 1976 with only three wells MIB-01, MIB-02 and MIB-03. The studies conducted in 2007, 2010 and 2016 aimed at re-conditioning some wells, resuming water injection and evaluating the remaining quantities of hydrocarbons in the upper Pinda reservoir. To date, the Mibale field has 20 wells including 14 producing wells and 6 injectors and an oil production of 5905 BOPD. Although crossing the reservoir layers containing more 365.1 MMstb of oils on 393 MMstbs of total field oils and activated by Gas-lift activation mode, the MIB-14ST2 has a very low oil output less than 100 BOPD, a well bottom pressure less than 450 psi and a high WOR of over 68%. After collecting field data and consulting works and related reports, we conducted the analysis and interpretation of field data using the simulation software of the hydrocarbon production system called IPM Prosper to identify the causes of the inefficiency of the production system. We understood that this well would produce at the bottom pressure of the zero well a flow rate of 464.978 bbl/day of oil, 30533.822 bbl/day of water and 12.29 stb/day/psi of productivity index. In view of this production capacity of the MIB-14ST2 well and the fluid characteristics of the reservoir and well, the optimization by conversion of the activation mode of the Gas-lift to ESP was applied. After analysis and interpretation of the results, the MIB-14ST2 well would be able to produce 75 Stb/day as oil flow; 4926.6 Stb/day as water flow and 0.022 MMscf/day. For production to take place after 11 minutes 9 seconds, the pump performance needs to be at 2218.06 ft with a frequency of 50 Hertz; the number of 76 stages; 1845.5 psig as suction pressure and 2641.9 Psig as discharge pressure. The total power of the system would be 118.4 hp with a total efficiency of 89.8% and 0.9% as a factor of engine power, which demonstrates that the system is efficient. In view of the results obtained, we note that the production of oil is still very low, which leads to further studies to review the depth of perforation of the well; make the material balance of the remaining reservoir fluids and the petrophysical characteristics of the layers crossing the MIB-14ST2 well. This research will contribute to the optimization of oil production in the upper Pinda reservoir and to a better understanding of its petrophysical behavior.

Keywords

Evaluation, Optimization, Conversion, Activation, Oil Well

1. Introduction

Applied in several research fields, optimization originated during World War II by the military in the field of applied mathematics research [1]. By involving multiple variables to find an optimal solution, optimization is a complex technique that has led to the resolution of previously unsolvable production problems [2]. Thus, production optimization refers to the various activities of measurement, analysis, modeling, prioritization, and implementation of actions aimed at improving the productivity of a field: reservoir, wells, and surface. It is a fundamental practice to ensure the recovery of developed reserves while maximizing yields [3].

Several solutions presented by optimization arise from two general methods called exact and approximate methods. These two methods are based on completely different principles applicable in hydrocarbon production. Each of them explores and exploits the search space according to its own techniques [4] [5].

However, in the case of production system optimization, this limit can be attributed to the complexity of the reservoir (reservoir geology, fluid characteristics, pressure, and temperature), geological uncertainty (accuracy of optimization study results), reservoir condition changes (the need for regular optimization reassessment), operational constraints (financial costs, etc.), environmental impacts, etc. [6].

In this regard, our study on optimization proposes a detailed analysis of well MIB-14ST2, focusing on the technical and operational aspects related to its production. The evaluation aims to better understand the well's performance, identify any potential issues (reservoir degradation, pressure losses, leaks, or other technical problems) that are limiting its production, and propose appropriate optimization solutions to enhance the well's production and efficiency. There are numerous methods and techniques for evaluating a production system, including production testing, pressure analysis, well logs, fluid analysis, reservoir modeling, and production monitoring. The choice of method depends on the evaluation objectives and the specific characteristics of the well [7]. In addition to these methods, the nodal analysis approach is used to analyze multiple fluid production problems in the well. It appears to be the best approach, because it quickly identifies the problem in a production system and proposes the optimal solution using one or more variables. This technique involves dividing the fluid flow path from the reservoir to the surface into two parts that meet at a point called the "node". Thus, the flow in the reservoir before the node is called "inflow", and in the well, it is referred to as "outflow" [8].

It should be noted that nodal analysis may be less suitable for complex production cases, such as multi-branch wells, water or gas injection wells, gas condensate reservoirs, etc., which is not the case for our well under study. In the case of multi-branch wells, fluid flows become more complex and interconnected, leading to variations in fluid flow rates and a non-steady flow regime. For injection wells, this introduces additional complexity due to changes in the composition of the injected fluids. Nodal analysis, however, is based on an isolated well assumption without interactions between wells, simple fluid flows, a stable flow regime, and struggles to accurately model the effects of different injected fluids on the overall production system.

If a nodal analysis has been conducted to evaluate well performance, it is entirely feasible to suggest enhanced oil recovery (EOR) methods, such as thermal injection, microbial injection, chemical injection, and gas injection. These EOR methods are selective based on the PVT properties of the fluids to be produced and the petrophysical characteristics of the reservoir [9].

Due to the complexity of solving the optimization problem in oil well production systems, computer simulation software is now being used to provide insights into the well's behavior under static and dynamic conditions [10] [11]. In this regard, IPM Prosper is the ideal software for conducting highly accurate simulations of well production systems.

1.1. Problem Statement

Given the low discovery of new oil and gas fields and the projected insufficiency in supply by 2025, it is imperative to invest in this sector as soon as possible and maximize the recovery of already discovered hydrocarbons using appropriate techniques [3].

The recovery methods are varied and depend on the reservoir characteristics, as well as the pressure, volume, and temperature properties of the reservoir fluids, the well activation method, and the surface collection network architecture. The upper Pinda formation, considered as the productive reservoir of the Mibale field, contains good-quality oil but with a pressure too low to lift it to the surface through production wells. Given this low pressure, after one year of production, gas-lift activation was implemented to improve production. Unfortunately, after one year, this activation method became ineffective, and the decision made by the operating company was to assist the reservoir by injecting water. However, due to corrosion issues with some water treatment equipment, the injection was halted in 2005, with an unsuccessful attempt to resume it in 2008.

In-depth studies conducted in 2007, 2010 and 2016 in the Mibale field led to the development of the field and the conversion of some wells' activation method to submersible electric pumps. However, the results were not as satisfactory as the company's expectations [12] [13]. This prompted a new line of thinking, which involved reviewing all the studies conducted in this field and identifying the shortcomings in order to propose appropriate solutions to the company for extracting a significant portion of the remaining 393 million stock tank barrels (MMstb) of oil in the upper Pinda reservoir.

Based on the above, we are interested in understanding the production system using nodal analysis approach in order to propose optimal solutions for increasing production in the Mibale field. This understanding raises the formulation of the following research questions:

- What is causing the low production yield of certain wells producing hydrocarbons from the upper Pinda reservoir in the Mibale field?
- Are the current gas-lift and submersible electric pump (ESP) activation methods used for oil production in the Mibale field still compatible with the economic and technical operating conditions of the associated wells?
- Do the petrophysical properties of the productive reservoir, upper Pinda, have a significant impact on the low oil production in this field?
- Is it necessary to convert the activation mode of MIBALE-14ST2 well abbreviated "MIB-14ST2 Well" based on the current knowledge in this field?

1.2. Specific Objectives

The specific objectives set in this study are as follows:

- Analyze and assess the production history of oil wells drilled in the Mibale field in order to identify strengths and weaknesses;
- Analyze the petrophysical properties of the upper Pinda reservoir and the parameters of the MIB-14ST2 well that crossed it;
- Develop IPR (Inflow Performance Relationship) and VLP (Vertical Lift Performance) curves and determine parameters related to the production of currently gas-lift activated well in order to optimize;

- Propose reconditioning works by converting the activation mode of MIB-14ST2 well.

1.3. Materials and Methods

For the realization of this study, we followed a methodological approach comprising two main phases.

1.3.1. Data Collection

Apart from documentary research, the following data were collected to the objectives set:

- Production fluid data from 2010 to 2021;
- Completion data (Casing depth, tubing depth, pump depth, inner and outer diameter, inclination, sediment level in the well, packer depth…);
- Reservoir pressure data (Gauge and perforation depth, gauge and perforation pressure, fluid gradient, pressure-depth relationship, limit depth for gauge pressure measurement, perforation pressure at the top of the reservoir, gauge temperature by depth…);
- Well testing data (Produced fluid rates, sediment rates, pressure and temperature at the wellhead, casing pressure, injected fluid rates, fluid production ratios…);
- Fluid and reservoir properties in initial and current conditions (Reservoir fluid viscosity, dissolved gas ratio, bubble pressure, reservoir pressure, reservoir permeability, oil and gas volumetric factor…);
- Reserve evaluation and simulation data of the upper Pinda reservoir in the Mibale field.

1.3.2. Data Processing and Interpretation of Results

Field data was processed for presentation in the form of tables, various graphs and maps. To do this, the following computer tools or software are used:

- Excel for the establishment of fluid production curves and mathematical or statistical calculations;
- Arcgis for the development of the study area map;
- Integrated Production Modelling-Production System Performance "IPM Prosper": to evaluate and optimize the Mibale field production system based on the analysis of the MIBALE-14ST2 producer well abbreviated "MIB-14ST2 Well".

The meaning of the results obtained from these treatments is the subject of the interpretation section. The following diagram (**Figure 1**) summarizes the phases of our methodological approach.

2. Overview of the Mibale Field and the MIB-14ST2 Well

The Congolese Offshore has 9 oil fields with 65 wells of which 21 wells belong to the Mibale field. Of these 21 wells, we have 14 producers, 6 injectors and 1 appreciation well, which is equivalent to 32.3% of the total oil fields. As of today,

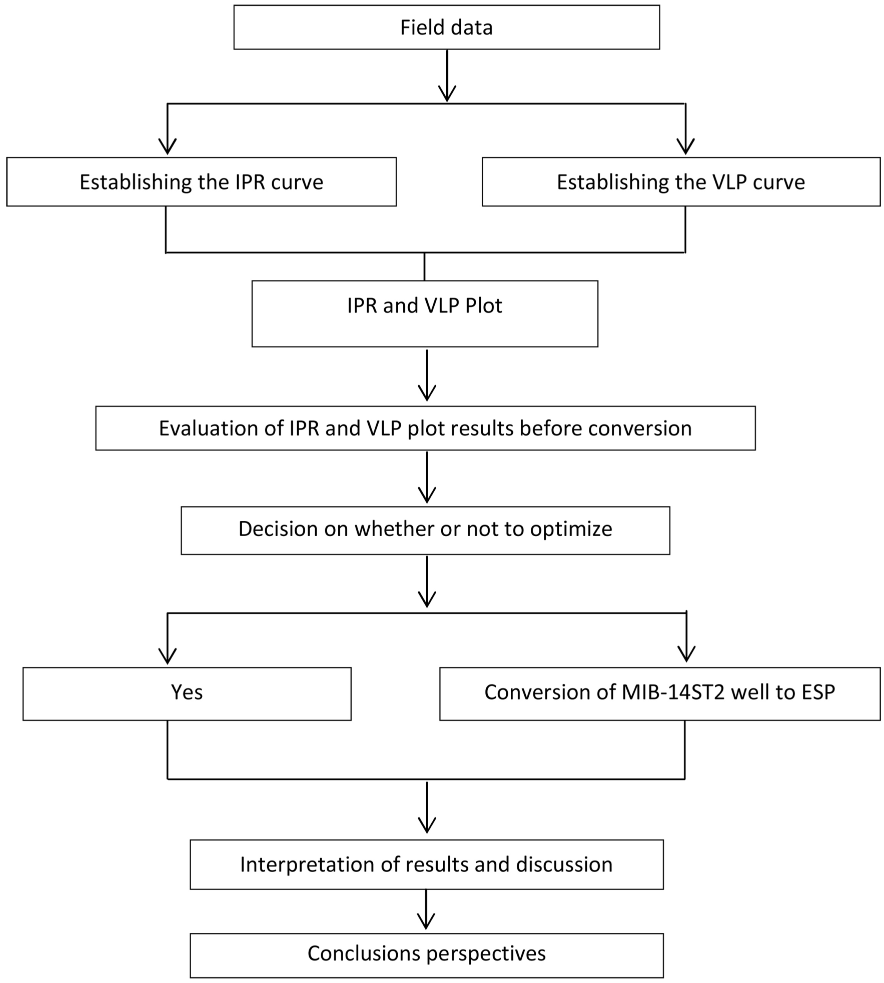

Figure 1. Methodological approach.

the field is producing an average of 5905.54 barrels of oil per day (BOPD) with a water-oil ratio (WOR) of over 60% (September 2021 average). Starting from the average official production of 25,000 BOPD for this company, we observe that this field contributes to the extent of 23.6%. Therefore, we can conclude that this field represents the largest offshore oil platform. It is worth noting that the Mibale field was discovered in 1973 by the oil company CHEVRON with the Mibale 1X well in the Upper Pinda formation, which is part of a fault-related structure with three branches. With three wells, MIB-01, MIB-02, and MIB-03, this field was put into production in 1976 [12] [13].

A good quality oil (32˚ API) has been discovered in a multi-layer complex in the upper part of the Albien-age Pinda formation, also known as the Upper Pinda reservoir. The Upper Pinda in the Mibale field is a reservoir with high permeability intervals, sand-rich layers, and dolomitic layers. It is divided into eight layers (LP or UP) ranging from the transition layer to L7 (UP-7). The upper transition layer is often described as poor-quality limestone and clays, while the underlying UP-1 layer consists of relatively low-quality limestone and less developed carbonate sands [8].

2.1. Location of the Mibale Field

The Mibale field is located in the coastal basin of the Democratic Republic of the Congo, 5 km wide and 3 to 7 km southeast of the DRC's offshore border with Cabinda (Angola), and covers an area of around 11 km² (**Figure 2**).

2.2. Reserves of Mibale Field

The studies conducted in 2016 provided the STOIIP (Stock Tank Oil Initially in Place) of the different layers of the Upper Pinda reservoir, as summarized in **Table 1** below, comparing them with the geological STOIIP values from 2006.

L1 layer (34%), L2 layer (22%) and L4 layer (25%) are the main STOIIPs. The L1 and L2 carbonate layer STOIIPs account for 56% of the Pinda field SToIIPs as a whole. The difference with the geological model lies mainly in the way water

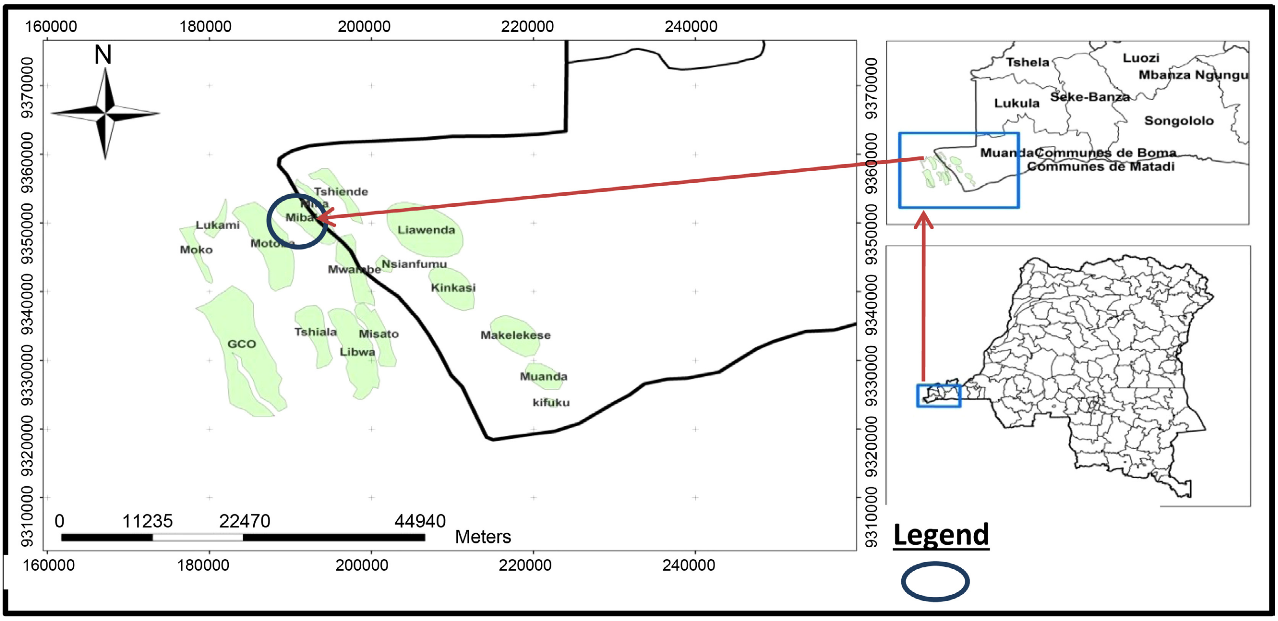

Figure 2. Location of Mibale field in the offshore of the coastal basin of the Democratic Republic of the Congo.

Table 1. Mibale field STOIIP by layer (MMstb).

Layer	Mibale Field	
	Geological model (2006)	Geological model (2016)
L1	97	132.3
L2	107	86.9
L3	74	46.9
L4	163	99
L5	13	7.7
L6	20	10.5
L7	22	9.7
STOIIP Total (MMstb)	**496**	**393**

saturation is used relative to depth, a relationship that introduces a large area of transition.

Table 2 shows the layers of the reservoir with the wells crossing them.

It is observed that well MIB-14ST2 penetrates layers L1, L2, L4, and L5. The amount of hydrocarbon reserves in these five layers amounts to 325.9 million stock tank barrels (MMstb).

2.3. Production of Mibale Field

The evolution of annual production in the Mibale field from 2010 to 2021 is illustrated in Figure 3. In 2010, the production was good, but in 2015, it was too low, indicating a rapid decline in production.

2.4. For MIB-14ST2 Well

The original MIB-14 well, which was drilled in July 1991, was completed in double sequence with a short sequence in the transition layer and a long sequence on the layers L1, L2 and L4. The MIB-14ST well was laterally followed to a TD of 7005 ftMD in May 1994 and was doubly completed in the TL layers (short sequence), L1, L2, L4, L5 and L6 (long sequence). In June 2007, total oil production was 1.7 MMSTB. Current production has 70 BOPD and a WOR of 68%.

Table 2. The layers of the reservoir with the wells crossing them.

Layer	Producing wells	Injector wells
L1	MIB-01-02-03-05-09ST-10-11-14-15-16-17-18	MIB-06-08-13ST
L2	MIB-01-02-03-05-09ST-10-11-14-15-16-17-18	MIB-06-13ST
L3	MIB-01-02-03	MIB-06
L4	MIB-02-05-09ST-14ST-10-11-15-16-18	MIB-07-08-12
L5	MIB-05-09ST-14ST-17	MIB-07-08-12
L6	MIB-09ST	MIB-07-08-12
L7		MIB-12

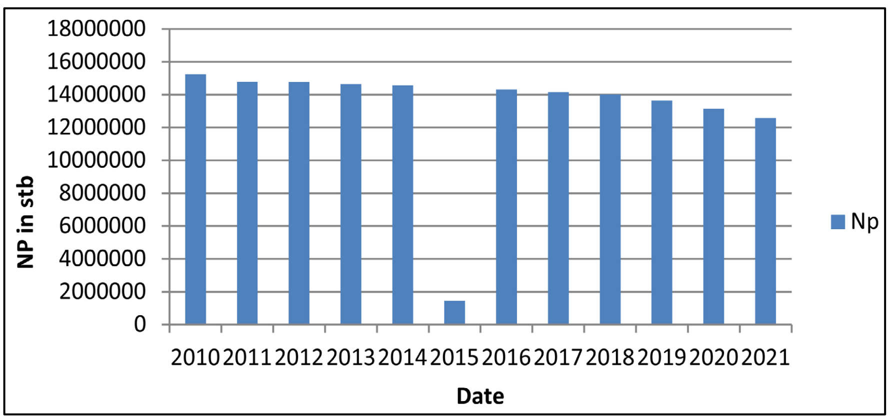

Figure 3. Butt diagram showing the evolution of oil production in the Mibale field from 2010-2021.

Note:

- The MIB-14 well means the fourteenth well of the Mibale field drilled vertically;
- The MIB-14ST well (Side Track) means the same fourteenth well of the Mibale field drilled vertically and then deviated;
- The MIB-14ST2 well means the same fourteenth well of the Mibale field drilled vertically and then deviated for a second time.

2.5. Information and Data Essential for Optimizing the MIB-14ST2 Well

Table 3 shows the reservoir and fluid properties of the Mibale field, in which all wells drain oil to surface.

Completion data for the MIB-14ST2 well are presented in Table 4 below.

Table 3. Reservoir and fluid parameters for the Mibale field [11] [14].

Parameter	Value
Bubble point pressure (Pb) @Tr	1336 psia
Drainage area	100 acres
Gas specific gravity (γ_g)	0.865
Impurities (N_2, CO_2, H_2S)	0
Initial gas formation volume factor (Bgi)	0.002 rb/scf
Initial oil formation volume factor (Boi)	1.13 rb/scf
Oil gravity (˚API) (γ_o)	32
Oil viscosity @Pb	1.1 cP
Overall heat transfer coefficient	8 btn/hr/F
Porosity ($\emptyset$)	18%
Recovery factor (RF)	32.58%
Reservoir permeability (k)	50 mD
Reservoir Pressure (Pr)	2600 psia
Reservoir temperature (Tr)	167˚F
Skin	0
Solution GOR (Rs)	300 scf/stb
Surface temperature	60˚F
Top node pressure	500 psig
Water salinity	0 ppm
Wellbore radius	0.354 ft

Table 4. Completion data for the MIB-14ST2 well on the Mibale field [8] [15].

Well type	Producing well
Trajectory	Vertical
Casing	Inside Diameter: 7 inches Outside Diameter: 9.625 inches Depth: 4877.5 feet
Tubing	Inside Diameter: 2992 inches Outside Diameter: 3.5 inches Depth: 5495.5 feet Inside Diameter: 3.958 inches Outside Diameter: 4.5 inches Depth: 4358 feet
Liner	Inside Diameter: 7 inches Depth: 5821 feet
BSW	98.5%
Perforation	431 feet

3. Results

There are many factors that can contribute to the reduction of pressure in a oil well production system, including [11] [12] [16] [17]:

1) Pipe friction: Pressure decreases can be caused by the friction between petroleum fluids and the pipe walls. They vary with the viscosity of the fluid, the internal diameter of the pipes, and the length of the pipes, and can increase if the pipes are too rough;

2) Narrows and obstructions: Narrows, bends or obstructions in production lines can lead to head losses. These losses are mainly caused by sudden changes in cross-section, which increase turbulence and fluid friction;

3) Clogging: Clogging of the well can lead to significant head losses. Solid particles, such as sands, clays or drilling cuttings, can settle in the well and obstruct fluid flow. This creates additional resistance to fluid flow and increases head losses;

4) Presence of water: If water is present in the well, it can cause high head losses. Water has a higher density than oil or gas, which increases the pressure required to move fluids through the well;

5) Cementing problems: Poor well cementing can lead to head losses. If the cement is not properly applied, or if there are leaks in the cementing, this can create undesirable flow paths for fluids, resulting in additional head losses;

6) Well activation mode restrictions: Limitations on the activation mode can be implemented in certain cases to control and pump the flow of trapped liquid in the well. This can be achieved through gas injection, valves, chokes, or other flow control devices. However, significant pressure losses can occur if these restrictions are too severe.

3.1. Wells before Activation Mode Conversion

3.1.1. Overview of MIB-14ST2 Well Design with Prosper Software

It should be remembered that the Prosper IPM software is a good simulator for converting from activation mode to ESP [18]. Data from **Table 4** (geothermal gradient, hole bottom equipment and tube and casing size data) were used as input data in IPM Prosper software to generate the MIB-14ST2 well architecture (**Figure 4**).

Figure 5 below shows us the perforation depths of MIB-14ST2 well.

3.1.2. Well Evaluation before Activation Mode Conversion

To assess the well's productivity, the IPR and VLP curves must be analyzed to determine the well's production capacity and operating point. To establish these curves, certain correlation choices must be made:

- Rs correlation;
- correlation on flow law;

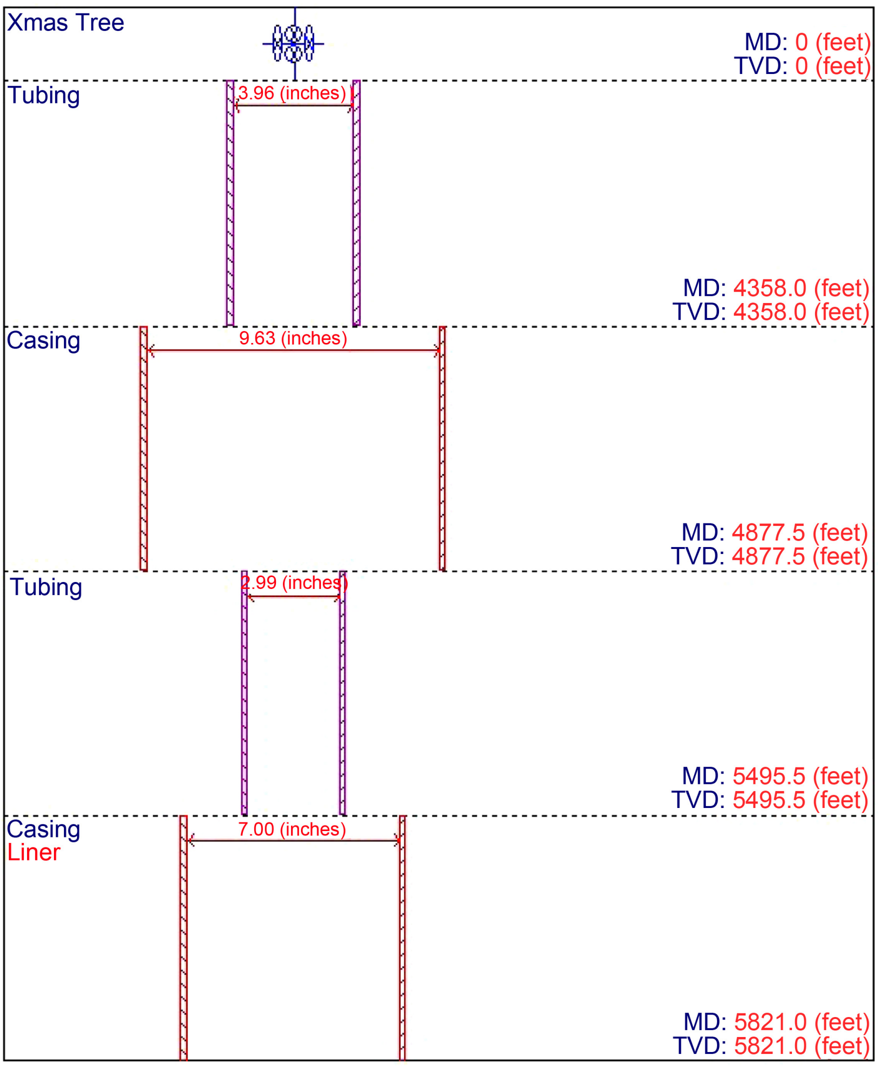

Figure 4. Bottom equipment configuration for MIB-14ST2 well.

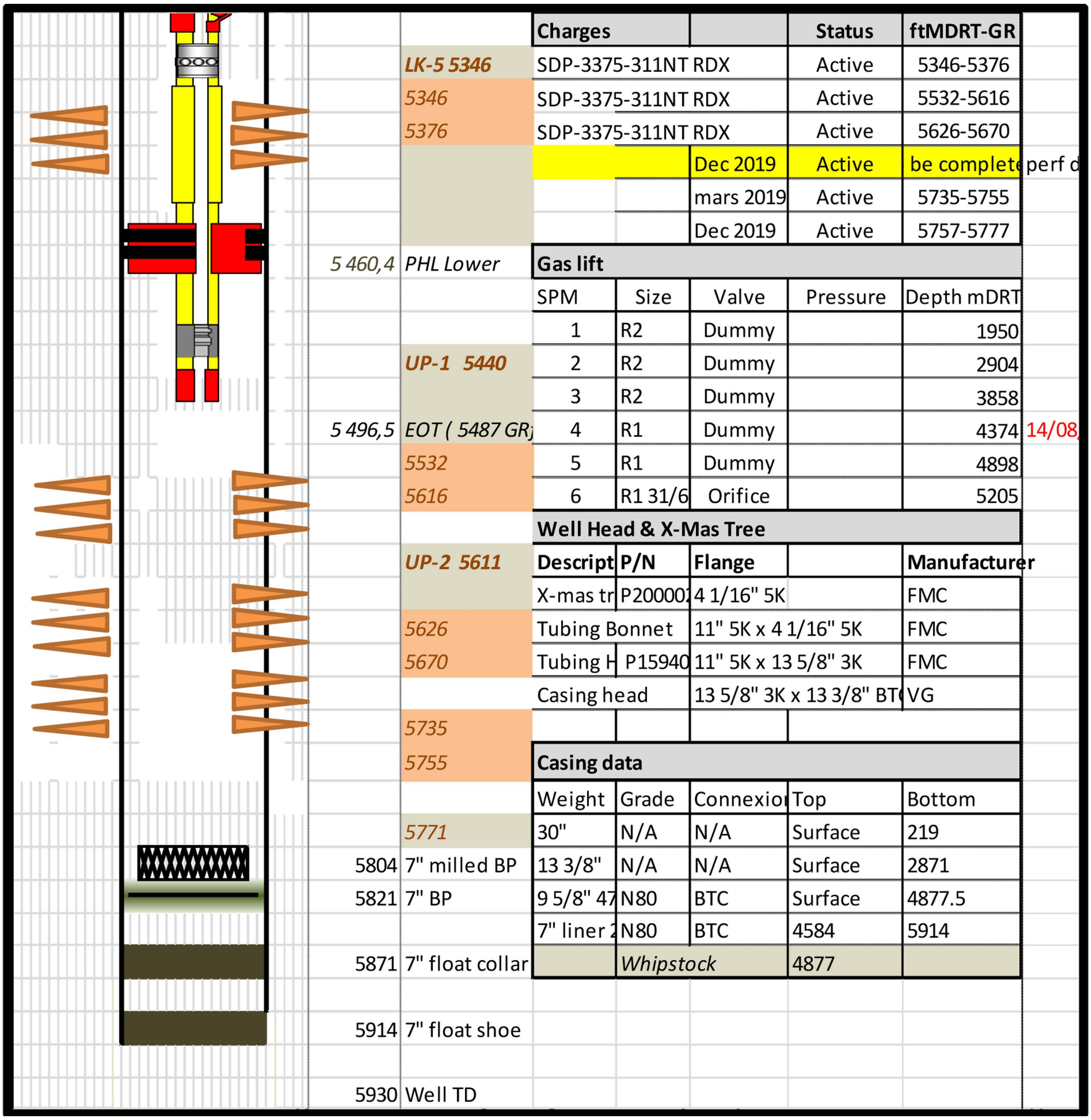

Figure 5. Illustration of perforation depths in MIB-14ST2 well.

- head loss correlation.

1) Choice of correlation to establish the IPR and VLP curves

a) Choice of gas solubility correlation (R_s)

To establish the IPR curve, we need to choose the dissolved GOR correlation. By replacing the fluid property values from Table 3 in mathematical Equations (1)-(5), we estimate the gas solubility (R_s) at bubble point pressure and compare this with the experimental value in terms of the absolute average error (AAE). The Rs's correlations expressed as mathematical equations are given as follows [16] [19]:

i) **Standing's (1981) correlation** is expressed in the following mathematical form:

$$R_s = c\left[\left(\frac{P}{18.2}+1.4\right)10^x\right]^{1.2048} \tag{1}$$

$$x = 0.0125\gamma_o - 0.00091(T-460)$$

ii) **Vasquez-Beggs correlation** is given in the following form:

$$R_s = C_1\gamma_{gc}P^{C_2}e^{\left[C_3 \cdot \frac{°API}{T+460}\right]} \tag{2}$$

with coefficient values C_1, C_2 et C_3.

iii) **Glaso correlation** is proposed according to this relation:

$$R_s = \gamma_g\left[\frac{API^{0.989}}{(T-460)^{0.172}} \cdot P_b^*\right]^{1.2255} \tag{3}$$

where $P_b^* = 10^x$ and $x = 2.8869 - [14.1811 - 3.3093\log P]^{0.5}$

iv) **Marhoun's correlation** proposed the following equation:

$$R_s = \left[a\gamma_g^b\gamma_o^c T^d P\right]^e \tag{4}$$

The coefficient values *a, b, c, d* and *e* are: a = 184.843208; b = 1.8778480; c = −3.1437; d = −1.32657 and e = 1.398441.

v) **Petrosky-Farshad correlation** is given by the following expression:

$$R_s = \left[\left(\frac{P}{112727}+12.34\right)\gamma_g^{0.8439} \cdot 10^x\right]^{1.73184} \tag{5}$$

$$X = 7.916\times10^{-4}\times API^{1.541} - 4.561\times10^{-5}(T-460)^{1.3911}$$

The following formula makes it possible to find the absolute average error (*AAE*):

$$AAE = \left|\frac{Vr - Vm}{Vr}\right| \times 100 \quad \text{as a percentage} \tag{6}$$

With *Vr*: Real Value (Field Data) and *Vm*: Measured Value (correlation values).

This allows us to summarize the R_s correlation values found with *AAE* (**Table 5**).

Table 5. Summary of R_s calculation using empirical correlations.

Correlation	R_s (*scf*/*STB*)	*AAE* (%)
Standing	645.5	115
Vasquez-Beggs	589.7	96.6
Glaso	339.37	13.12
Marhoun	435.51	45.1
Petrosky-Farshad	599.4	99.8

We note that the value of GOR dissolved in oil (R_s) calculated by the Glaso correlation is a little close to that of the Mibale Field determined by PVT analyses with a deviation or AAE of 13.12%, which allows us to choose this correlation as the one applicable in the optimization of this well. Referring to **Table 3**, the value of Rs is 300 scf/stb and using the Glaso correlation, R_s is 339.37 scf/stb with 13.12 deviation factor.

b) Choice of flow law correlations

Several correlations on the flow law in the reservoir have been established with their mathematical expressions [5] [20] [21]. These are the correlations of:

- Darcy's method or law;
- Vogel's method;
- IP method;
- Fetkovich method;
- Johns, Blout and Glaze method.

Given the available data and the characteristics of the Mibale field reservoir, Darcy's law correlation was used to establish the IPR curve. The mathematical expression of Darcy's law is as follows:

$$Q_o = \frac{0.0078 \times k \times h\left(P_r - P_{wf}\right)}{\mu_o B_o \ln\left(\frac{r_e}{r_w}\right)} \tag{7}$$

c) Choice of upward two-phase flow correlation

Several correlations on the law of flow in the reservoir have been established with their mathematical expressions. Beggs and Brill summarized the correlations of the law of flow into three main categories, each of which varies in complexity and technique. These are the following categories [22]:

Category A: No slip effect or flow regime is considered—Poettmann & Carpenter, Fancher & Brown;

Category B: Slip effect is considered, no flow regime is considered—Hagedorn & Brown, Gray;

Category C: Both slip effect and flow regime are considered—Beggs & Brill, Orkiszewski, Duns & Ros.

However, no single correlation was found to be the best over the others for all flow conditions. Individual well tests and experience can be used to obtain the correlation that best suits the characteristics of each well [23] [24]. Some of these correlations are given in the following mathematical form:

i) **Poettman and Carpenter's correlation** is a semi-empirical method using the general energy equation and considering the mixture of oil, gas and water as single-phase.

ii) **Hagedorn and Brown's correlation** is an extension of Poettmann and Carpenter's.

iii) **Beggs and Brill's correlation** studied head losses in tubing using the same technique, as for horizontal pipes, with the introduction of a factor that takes into account the inclination, which changes from −90˚ to +90˚. This method is based on determining the flow regime, which depends on Hold up, the pressure gradient, the Froude number.

After inputting values in the software for the pressure at the wellhead, water cut, oil or liquid flow rate, gas-oil ratio (GOR), various depths of the well down to the tubing, and the pressures prevailing in the well, the Prosper software calculates correlation parameters by determining the deviation factor for each correlation. The obtained values are depicted in Figure 6 and Figure 7.

Correlation	Parameter 1	Parameter 2	Standard Deviation
Duns and Ros Modified	0.77081	0.76237	212.677
Hagedorn Brown	0.76804	0.77012	212.154
Fancher Brown	0.77412	0.77154	212.997
Mukerjee Brill	0.7676	0.76779	213.445
Beggs and Brill	0.76661	0.74658	212.174
Petroleum Experts	0.76799	0.77004	212.178
Orkiszewski	0.76804	0.77012	212.154
Petroleum Experts 2	0.76799	0.77004	212.178
Duns and Ros Original	0.77415	0.74647	213.139
Petroleum Experts 3	0.76799	0.77004	212.178
GRE (modified by PE)	0.77108	0.76846	213.211
Petroleum Experts 4	0.76892	0.77123	212.411
Hydro-3P	0.77961	0.77422	211.155
Petroleum Experts 5	0.76801	0.77021	212.153
OLGAS 2P	1.8276	1.8276	180.465
OLGAS 3P	1.8276	1.8276	180.465
OLGAS3P EXT	1.8276	1.8276	180.465

Figure 6. Tubing correlation parameters.

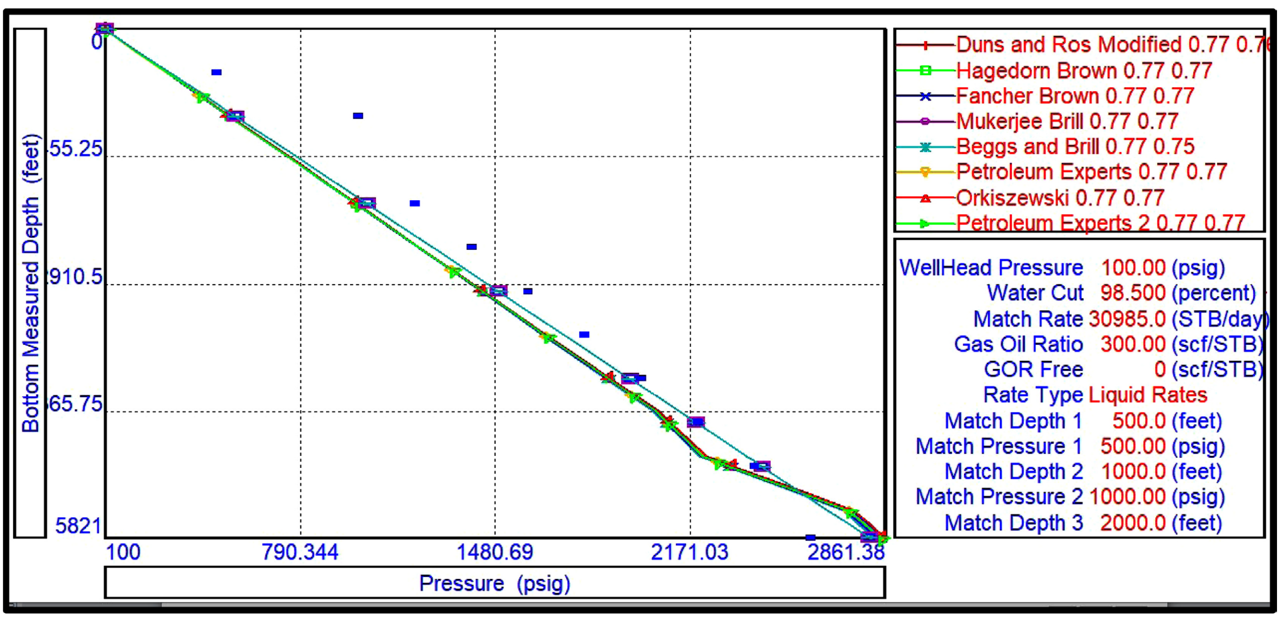

Figure 7. Pressure gradient curves and depth for different upward two-phase flow correlations. Note: The Poettman and Carpenter's correlation is not included in the Prosper IPM software because it is corrected by the Hagedorn and Brown's Correlation.

In view of Figure 7 below, it is noted that each correlation has a relative error but it is found that the Beggs and Brill correlations are the most appropriate for calculating outflow load losses because the values of two parameters have a small value (0.74) with a small deviation factor of 212.174 compared to that of other correlations that are greater than 0.76.

2) Establishing the IPR and VLP curves

Unlike manual calculations and other optimization software, IPM Prosper was used to model the well in different scenarios to obtain accuracy on the actual well performance. This modeling was based on Darcy's law and the data from Table 3 to establish the IPR (Inflow Performance Relationship) and the Beggs and Brill correlation, combined with data from the pressure at the upper node, GOR (Gas-Oil Ratio), and a 98.5% water cut.

Figure 8 illustrates the pressure and fluid flow rates values found after the calculations.

After plotting the IPR and VPL curves for the MIB-14ST2 well, it can be seen in Figure 9 that an absolute maximum flow rate "AOF" of 30998.8 stb per day should be produced with the IP of 12.29 stb per day per psi. Unfortunately, the IPR curve is a steep slope, demonstrating that this well was producing absolutely nothing, and there is no point of contact between the two curves.

3) Well sensitivities

Considering that the variables for the MIB-14ST2 well are the water cut, the pressure at the upper node, and the GOR, we varied the GOR from 0 to 1000 scf/stb the first node pressure from 500 to 2600 psig and the water cut from 0 to 100%.

Figure 10 illustrates the calculations performed taking into account the values of the variables listed above.

As we described in the problem, the production of the MIB-14ST2 gas-lift activated well is almost zero or too low so according to our study case, we do the sensitivity of variables such as the first node pressure, the water cut and the GOR to see if there will be a possibility to convert the activation mode.

Liquid Rate	Oil Rate	VLP Pressure	IPR Pressure	dP Total Skin	dP Perforation	dP Damage	dP Completion	Completion Skin	dP Sand Control	Sand Control Skin	Total Skin	WellHead Pressure	WellHead Temperature	dP Friction	dP Gravity
(STB/day)	*(STB/day)*	*(psig)*	*(psig)*	*(psi)*	*(psi)*	*(psi)*	*(psi)*		*(psi)*			*(psig)*	*(deg F)*	*(psi)*	*(psi)*
31.0	0.46535	3000.82	2597.48	0	0	0	0	0	0	0	0	500.00	61.00	0.0051167	2500.81
1660.9	24.9	2981.36	2464.90	0	0	0	0	0	0	0	0	500.00	105.41	4.48	2476.88
3290.8	49.4	2984.41	2332.33	0	0	0	0	0	0	0	0	500.00	126.30	15.54	2468.87
4920.6	73.8	2997.75	2199.75	0	0	0	0	0	0	0	0	500.00	136.83	32.74	2465.01
6550.5	98.3	3018.75	2067.18	0	0	0	0	0	0	0	0	500.00	143.07	55.98	2462.77
8180.4	122.7	3046.53	1934.61	0	0	0	0	0	0	0	0	500.00	147.18	85.18	2461.34
9810.3	147.2	3080.70	1802.03	0	0	0	0	0	0	0	0	500.00	150.10	120.33	2460.37
11440.1	171.6	3121.08	1669.46	0	0	0	0	0	0	0	0	500.00	152.26	161.40	2459.69
13070.0	196.0	3167.56	1536.88	0	0	0	0	0	0	0	0	500.00	153.94	208.37	2459.20
14699.9	220.5	3220.08	1404.29	0	0	0	0	0	0	0	0	500.00	155.27	261.23	2458.84
16329.7	244.9	3278.58	1271.54	0	0	0	0	0	0	0	0	500.00	156.36	319.99	2458.60
17959.6	269.4	3343.05	1138.54	0	0	0	0	0	0	0	0	500.00	157.26	384.63	2458.42
19589.5	293.8	3413.45	1005.19	0	0	0	0	0	0	0	0	500.00	158.03	455.14	2458.31
21219.4	318.3	3489.77	871.28	0	0	0	0	0	0	0	0	500.00	158.68	531.51	2458.26
22849.2	342.7	3572.00	736.16	0	0	0	0	0	0	0	0	500.00	159.24	613.76	2458.24
24479.1	367.2	3660.13	594.15	0	0	0	0	0	0	0	0	500.00	159.73	701.86	2458.27
26109.0	391.6	3754.14	446.45	0	0	0	0	0	0	0	0	500.00	160.17	795.82	2458.32
27738.8	416.1	3854.03	298.75	0	0	0	0	0	0	0	0	500.00	160.55	895.63	2458.40
29368.7	440.5	3959.79	151.05	0	0	0	0	0	0	0	0	500.00	160.89	1001.29	2458.50
30998.6	465.0	4071.42	2.27	0	0	0	0	0	0	0	0	500.00	161.20	1112.80	2458.62

Figure 8. Calculation results for pressure and flow rate parameters for IPR and VLP curves.

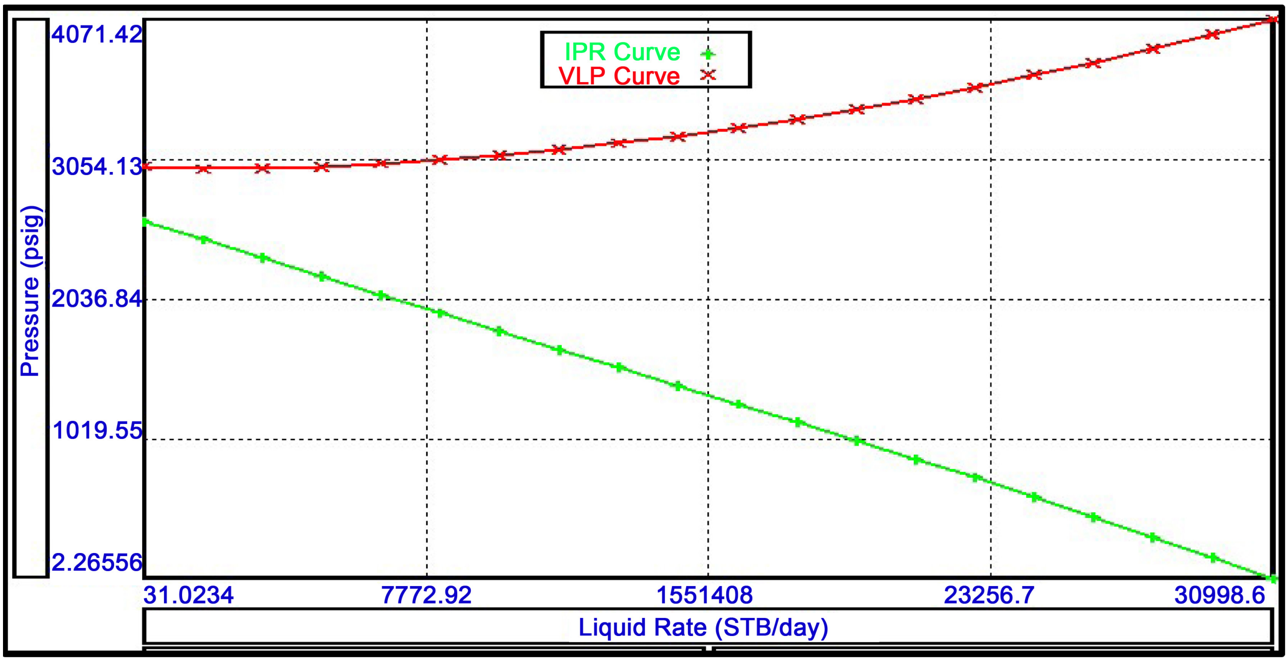

Figure 9. IPR and VLP curves for MIB-14ST2 well.

Water Cut	10.000	*(percent)*
Gas Oil Ratio	333.33	*(scf/STB)*
First Node Pressure	966.67	*(psig)*

Liquid Rate	Oil Rate	VLP Pressure	IPR Pressure	dP Total Skin	dP Perforation	dP Damage	dP Completion	Completion Skin	dP Sand Control	Sand Control Skin	Total Skin	WellHead Pressure	WellHead Temperature	dP Friction	dP Gravity
(STB/day)	*(STB/day)*	*(psig)*	*(psig)*	*(psi)*	*(psi)*	*(psi)*	*(psi)*		*(psi)*			*(psig)*	*(deg F)*	*(psi)*	*(psi)*
31.0	27.9	3048.43	2597.61	0	0	0	0	0	0	0	0	966.67	60.54	0.016895	2081.75
1660.9	1494.8	3017.91	2472.14	0	0	0	0	0	0	0	0	966.67	88.10	6.24	2044.65
3290.8	2961.7	3014.36	2346.67	0	0	0	0	0	0	0	0	966.67	107.85	20.92	2026.63
4920.6	4428.6	3026.35	2221.20	0	0	0	0	0	0	0	0	966.67	120.33	43.03	2016.60
6550.5	5895.5	3049.80	2095.73	0	0	0	0	0	0	0	0	966.67	128.62	72.31	2010.83
8180.4	7362.3	3082.51	1970.27	0	0	0	0	0	0	0	0	966.67	134.46	108.52	2007.33
9810.3	8829.2	3123.47	1844.80	0	0	0	0	0	0	0	0	966.67	138.78	151.53	2005.24
11440.1	10296.1	3172.10	1719.33	0	0	0	0	0	0	0	0	966.67	142.09	201.21	2004.13
13070.0	11763.0	3228.03	1593.67	0	0	0	0	0	0	0	0	966.67	144.72	257.47	2003.70
14699.9	13229.9	3291.00	1462.10	0	0	0	0	0	0	0	0	966.67	146.85	320.22	2003.81
16329.7	14696.8	3360.82	1320.21	0	0	0	0	0	0	0	0	966.67	148.60	389.38	2004.32
17959.6	16163.7	3437.33	1164.74	0	0	0	0	0	0	0	0	966.67	150.08	464.89	2005.16
19589.5	17630.5	3520.31	990.23	0	0	0	0	0	0	0	0	966.67	151.34	546.79	2006.06
21219.4	19097.4	3609.77	786.14	0	0	0	0	0	0	0	0	966.67	152.42	634.98	2007.14
22849.2	20564.3	3705.64	525.80	0	0	0	0	0	0	0	0	966.67	153.37	729.38	2008.40
24479.1	22031.2	3807.84	33.37	0	0	0	0	0	0	0	0	966.67	154.20	829.96	2009.80
26109.0	23498.1	3916.29	-990.00	0	0	0	0	0	0	0	0	966.67	154.93	936.67	2011.31
27738.8	24965.0	4030.98	0	0	0	0	0	0	0	0	0	966.67	155.59	1049.74	2012.67
29368.7	26431.8	4151.87	0	0	0	0	0	0	0	0	0	966.67	156.17	1168.97	2014.09
30998.6	27898.7	4278.94	0	0	0	0	0	0	0	0	0	966.67	156.70	1294.29	2015.58

Figure 10. Illustration of one of the sensitivity calculation tables for variables Water cut, GOR, and First Node pressure.

After the sensitivity of these variables, we notice that the IPR and VLP curves intercept at several points between which we can get a realistic point of operation (Figure 11).

3.2. ESP Optimization of the MIB-14ST2 Well

3.2.1. Well Design

Optimization by activation mode conversion of the MIB-14ST2 well is considered in this type of well to be the best activation mode capable of compensating

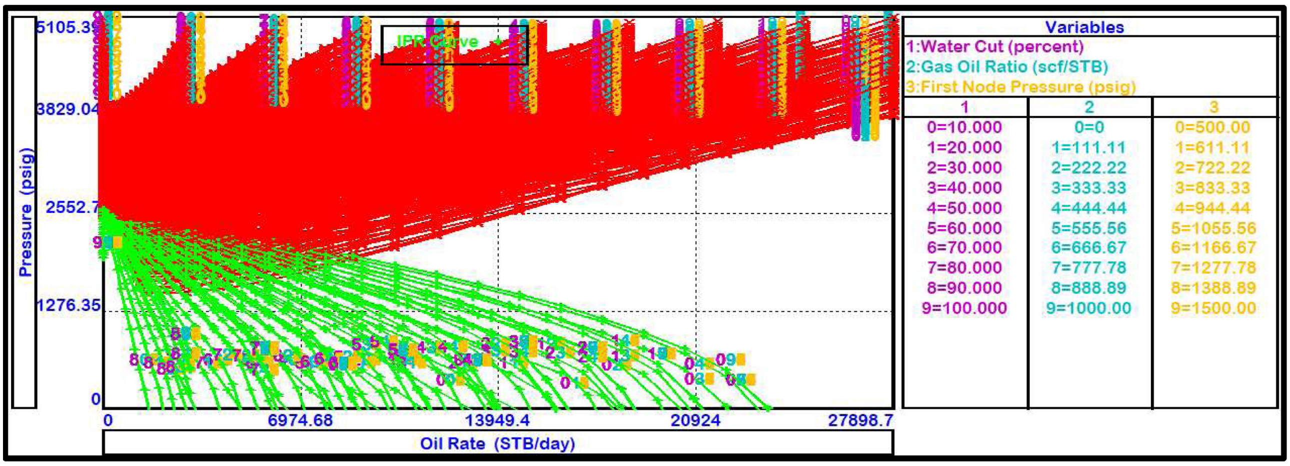

Figure 11. Sensitivity analysis curves for well MIB-14ST2.

for the loss of pressure due to the high liquid rate and low gas flow rate according to the evaluation made in this well. The pump also has operational constraints for its functioning, namely [25] [26]:

- Limit or maximum power;
- Operating zone or map the pump's performance;
- The reservoir suction pressure must be higher than the bubble pressure because gas is not allowed in the pump as it is designed only to handle liquids.

Taking into account these different constraints, the dynamic water level in the well, the desired oil flow rate, the number of stages, engine power and cable length, we have the well design as shown in **Figure 12** below.

3.2.2. Pump Operation after Design

Taking into account **Figure 12** of the design, the IPM Prosper software performs calculations using integrated equations, giving precision on the number of stages, pump efficiency and real power (Equations (8)-(11)). If the flow rate produced exceeds the maximum flow rate, pump efficiency becomes low. Also, a high power factor in a pump is important because it improves energy efficiency, maintains the stability of the electrical network, improves pump performance and reduces operating costs, as is the case with the MIB-14ST2 well. The mathematical formulae for the pump parameters mentioned above are as follows [25]:

- The total dynamic head (TDH) for the ESP system is defined as the pressure head immediately above the pump (in the tubing) given in the following mathematical form and expressed in feet:

$$TDH = H_d + F_t + P_d \tag{8}$$

- The discharge pressure is given by the following expression:

$$PDP = THP + GAVG \cdot TVDP,\ psia \tag{9}$$

- Hydraulic power is:

$$P_{HYD} = \frac{Q \times h \times \rho \times g}{n_h}\text{, kilowatts} \tag{10}$$

Pump Depth (Measured)	5000.0	*(feet)*
Operating Frequency	50.00	*(Hertz)*
Maximum Pump OD	6.00	*(inches)*
Length Of Cable	5000.0	*(feet)*
Gas Separator Efficiency	0	*(percent)*
Number Of Stages	76	
Voltage @ Surface	2127.68	*(Volts)*
Pump Wear Factor	0	*(fraction)*

Pump	CENTRILIFT - GC6100	
Motor	Boret - EDB125-117B5	
Nameplate Power	168.00	*(hp)*
Nameplate Voltage	2100.00	*(Volts)*
Nameplate Current	49.00	*(amps)*
Cable	#1 Aluminium	

Figure 12. Photo showing the design interface on wells MIB-14ST2.

With:

- ✓ Q: fluid flow in cubic meter per second
- ✓ H: Manometric height in meters
- ✓ ρ: mass volume in kilograms per cubic meter
- ✓ g: gravity in meters per square second
- ✓ n_h: hydraulic efficiency, decimal (Between 0 and 1)
- Hydraulic efficiency (n_h) is a measurement made in a radial flow stage and the flow always follows the contour:

$$n_h = \frac{\Delta P \cdot q_{inlet}}{P_h} \tag{11}$$

With:

- ✓ q_{inlet}: total liquid flow in the pump, in cubic meter per second
- ✓ ΔP: ESP pump pressure differential to overcome head losses between bottom and top of well, in psia
- Total system efficiency:

$$\eta_{TOT} = \eta_{PUMP} \cdot \eta_{SEAL} \cdot \eta_{MOTOR} \cdot \eta_{CABLE} \cdot \eta_{TRANS} \cdot \eta_{DRIVE} \text{, in decimal} \tag{12}$$

With:

- ✓ η_{CABLE} : cable efficiency approx. 95% may also be lower with longer cable and higher amperage
- ✓ η_{MOTOR} : motor efficiency: most suppliers say 90% for induction motors, but

more realistically 80% to 90%

- ✓ η_{PUMP} : pump efficiency from 20% to 80%
- ✓ η_{SEAL} : protector efficiency very close to 100%
- ✓ η_{TOT} : total system efficiency typically 20% to 60%
- ✓ η_{TRANS} : transformer typically 98% to 99%
- ✓ η_{DRIVE} : 95% dimmer for low voltage VSD and 100% dimmer for electrical panel

- The power of the system:

$$P_{SYS} = \frac{P_{HYD}}{\eta_{TOT}} \text{ in horsepower} \tag{13}$$

- Power factor:

$$PF = \frac{kW}{kVA} \tag{14}$$

In decimal (Between 0 and 1)

With:

- ✓ kVA: apparent power, kilowatt
- ✓ kW: real power, kilowatt

The results obtained for the entire pumping system are as follows (**Figure 13**):

- 76 stages with a pump power requirement of 106.6 hp and motor efficiency of 87.14% (**Figure 11**).

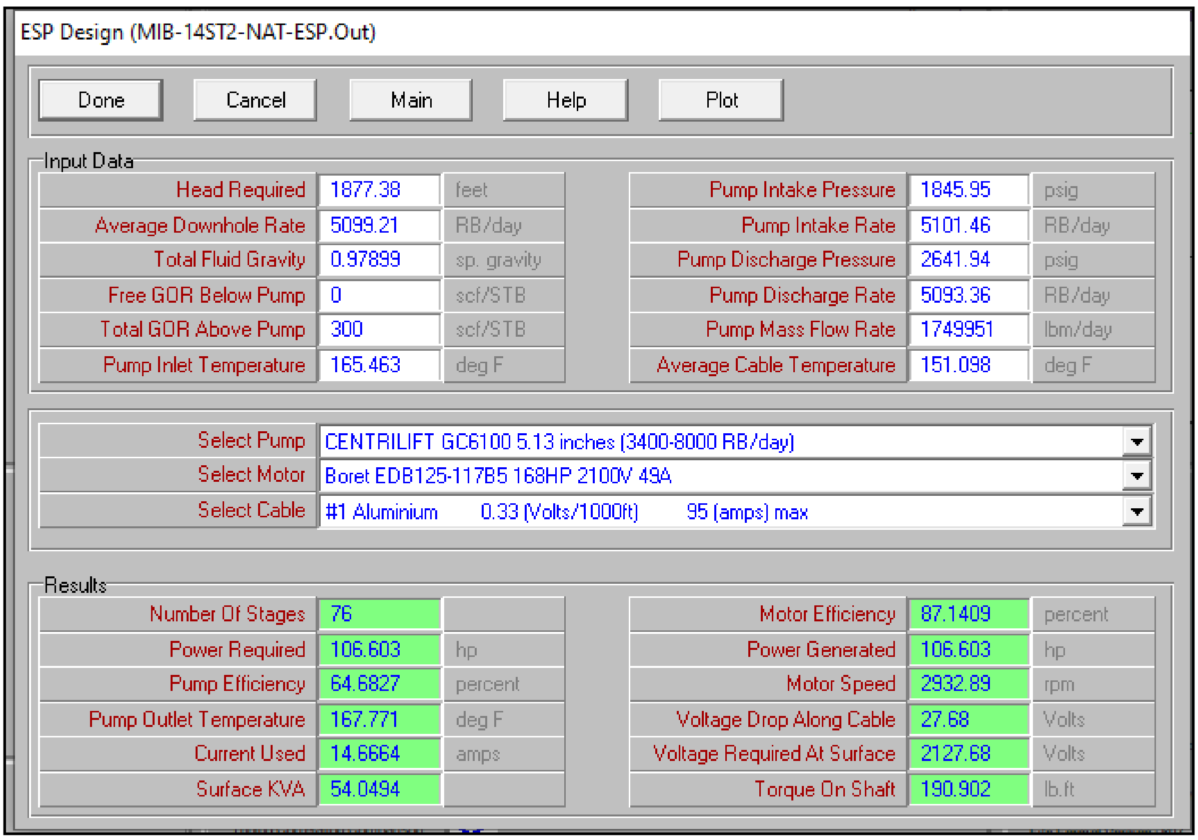

Figure 13. Photo showing the result interface after MIB-14ST2 well design.

Using Equations (12)-(14), we find:

- ✓ n_{total}: 89.8%
- ✓ The power of the system: 118.04 hp
- ✓ Power factor: 0.90

With these different values obtained for total efficiency, power factor and system power, we can see that the system's total efficiency is good, as it exceeds 60% according to the criteria for good operation. Also, the power factor is above 80%, which proves that there will be no considerable or high voltage requirement during production, and that friction between fluids is reduced, thus reducing load losses. Considered as the surface electrical power, the value of the system power obtained is higher than that which we want to apply to the fluid in order to compensate for dissipation, thus increasing fluid velocity and reducing head losses by elevation.

3.2.3. ESP Performance for the MIB-14ST2 Well

The pump's performance is delimited in a zone called the operational zone, in which the pump can operate with minimum and maximum frequency [17].

The performance curve of the ESP pump can change based on the molecular weight of the gas and the inlet fluid temperature. We note that the molecular weight of the gas can influence the overall viscosity of the fluid which will lead to a change in fluid flow properties through the ESP pump, which can affect its overall efficiency and performance. And also if the gas in the pumped fluid reaches steam pressure, it can create gas pockets that can cause cavitation of the pump which could damage the pump and reduce its efficiency.

To avoid making corrections to this curve, the following formula is used:

$$\Delta h = \frac{P_{out} - P_{in}}{\rho_{mix} \times g} \tag{15}$$

When expressing performance in terms of head (Δh), the unit used is feet. The density of the fluid mixture (ρmix) is also an important parameter to consider in calculating head.

- ✓ P_{out}: Outlet pressure (in psi); P_{in}: Inlet pressure (in psi);
- ✓ ρ_{mix}: Density of the fluid mixture (in lb/ft3);
- ✓ g: Acceleration due to gravity (32.2 ft/s2).

Thus, the pump's head required is based on the depth of its location, while that of well MIB-14ST2 is at 1877.38 feet after simulation and would give 5083.94 stb/d as liquid flow. This pump will operate with a frequency of 50 Hertz and on the best efficiency line (BEL), we obtain the pump's best efficiency point at 64.72% (**Figure 14**).

Referring to the formula for discharge pressure, we derive the gradient average of the fluid at the pump location:

$$GAVG = \frac{PDP - THP}{TVD\ PUMP} \tag{16}$$

With:

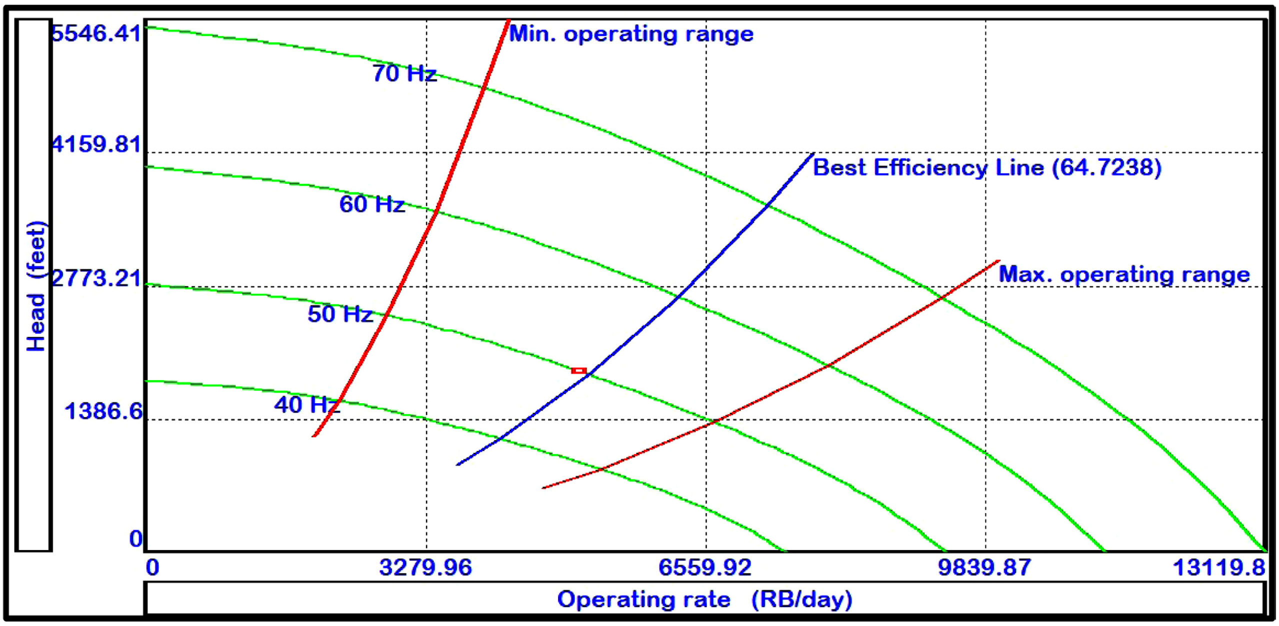

Figure 14. Determination of pump performance zone for MIB-14ST2 well.

- ✓ *TVD PUMP*: vertical depth for pump installation, feet
- ✓ *PDP*: pump discharge pressure, psia
- ✓ *GA VG*: average fluid gradient, psi/feet
- ✓ *THP*: pressure at the tubing head, psia

Using the Equation (16) and the pressure at the head of the MIB-14ST2 well at 90 psig, we obtain 0.499 psi/ft as the average fluid gradient at the depth of the pump installation; this also confirms the dynamic level of the water according to the filling data of this well because the average water gradients are equal to or greater than 0.4 psi/ft.

3.2.4. Variable Sensitivities in the MIB-14ST2 Well after ESP Installation

Concerning sensitivities to frequency and number of stages, we have performed several scenarios by plotting the IPR and VLP performance curves with variables such as pump frequency from 30 to 70 Hertz, number of stages from 10 to 100 stages and water cut from 10% to 100%.

After several scenarios, the results are presented in 2 ways in a graphical form (Figure 16) showing the well operating points from the intersection of the IPR and VLP curves and in a numeric form (Figure 15) showing each scenario with its fluid production rates. Considering variable values, several tables have been presented but in this work, we present only one to illustrate this.

We note that there are several operating points in this well, demonstrating that this well can still produce after conversion of the activation mode (Figure 16).

3.2.5. Oil Production in the MIB-14ST2 Well after Installation of the ESP Pump

From the analysis and interpretation of Figures 9-12 we obtained the operating

Number of Stages	50	
Operating Frequency	34.44	(Hertz)
Water Cut	50.000	(percent)

Liquid Rate	Oil Rate	VLP Pressure	IPR Pressure	dP Total Skin	dP Perforation	dP Damage	dP Completion	Completion Skin	dP Sand Control	Sand Control Skin	Total Skin	WellHead Pressure	WellHead Temperature	dP Friction	dP Gravity	Pump Intake Pressure	Pump Discharge Pressure
(STB/day)	(STB/day)	(psig)	(psig)	(psi)	(psi)	(psi)	(psi)		(psi)			(psig)	(deg F)	(psi)	(psi)	(psig)	(psig)
31.0	15.5	2590.54	2597.48	0	0	0	0	0	0	0	0	500.00	60.75	0.010645	2436.05	2251.95	2585.29
1660.9	830.4	2369.30	2464.90	0	0	0	0	0	0	0	0	500.00	96.46	4.35	2181.46	2145.30	2445.73
3290.8	1645.4	2351.92	2332.33	0	0	0	0	0	0	0	0	500.00	117.26	14.64	2152.85	2015.26	2236.97
4920.6	2460.3	2355.26	2199.75	0	0	0	0	0	0	0	0	500.00	128.95	30.23	2140.23	1883.71	1993.55
6550.5	3275.3	2369.91	2067.18	0	0	0	0	0	0	0	0	500.00	136.27	50.85	2133.91	1751.73	1751.79
8180.4	4090.2	2392.63	1934.61	0	0	0	0	0	0	0	0	500.00	141.25	76.34	2130.75	1619.57	1619.63
9810.3	4905.1	2422.03	1802.03	0	0	0	0	0	0	0	0	500.00	144.85	106.57	2129.45	1487.33	1487.39
11440.1	5720.1	2457.15	1669.46	0	0	0	0	0	0	0	0	500.00	147.58	141.53	2128.63	1355.43	1355.49
13070.0	6535.0	2497.91	1536.88	0	0	0	0	0	0	0	0	500.00	149.70	180.93	2127.51	1224.99	1225.05
14699.9	7349.9	2543.80	1403.69	0	0	0	0	0	0	0	0	500.00	151.41	224.79	2124.77	1096.16	1096.22
16329.7	8164.9	2594.51	1265.14	0	0	0	0	0	0	0	0	500.00	152.82	273.05	2120.25	964.12	964.18
17959.6	8979.8	2649.78	1118.50	0	0	0	0	0	0	0	0	500.00	153.99	326.03	2111.39	827.88	827.94
19589.5	9794.7	2709.67	960.21	0	0	0	0	0	0	0	0	500.00	154.98	382.98	2098.50	684.61	684.66
21219.4	10609.7	2773.92	782.99	0	0	0	0	0	0	0	0	500.00	155.83	444.18	2077.75	530.20	530.25
22849.2	11424.6	2842.52	565.65	0	0	0	0	0	0	0	0	500.00	156.57	510.56	2039.62	352.22	352.25
24479.1	12239.6	2915.22	118.48	0	0	0	0	0	0	0	0	500.00	157.22	587.85	1902.14	37.30	37.31

Figure 15. Illustration of the numerical sensitivity results of the Frequency, Stages Number and Water cut variables (50 Stages, 34.4 Hertz and 50% Water cut).

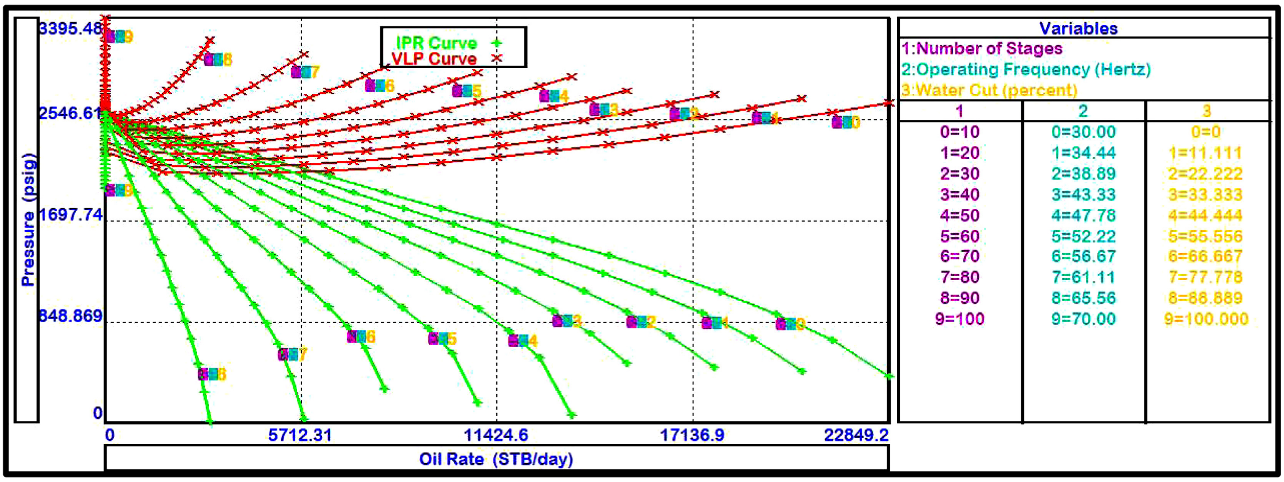

Figure 16. Sensitivity analysis of pump frequency, number of pump stages and water cut for well MIB-14ST2.

point from the IPR and VLP plot. This new point was used to determine the new production of the MIB-14ST2 well (Figure 17):

- After several scenarios involving the change of different pump types according to flow rates and other variables such as frequency, motor efficiency, etc.; the simulation showed that the well has the capacity to produce 464.978 stb/day of oil but the realistic point of operation gives us unsatisfactory results with an oil output of 75 stb/d and a water flow of 4926.6 and gas of 0.02 MMscf.

This result then leads to a study on the re-evaluation of the fluids in place in the reservoir and the reconditioning of the well (revising the perforation depth and the quantity of water in the different layers crossed).

Looking at Table 1 and Table 2, we can see that the MIB-14ST2 well crosses the L1, L2, L4 and L5 layers, the last of which has a high permeability but a very

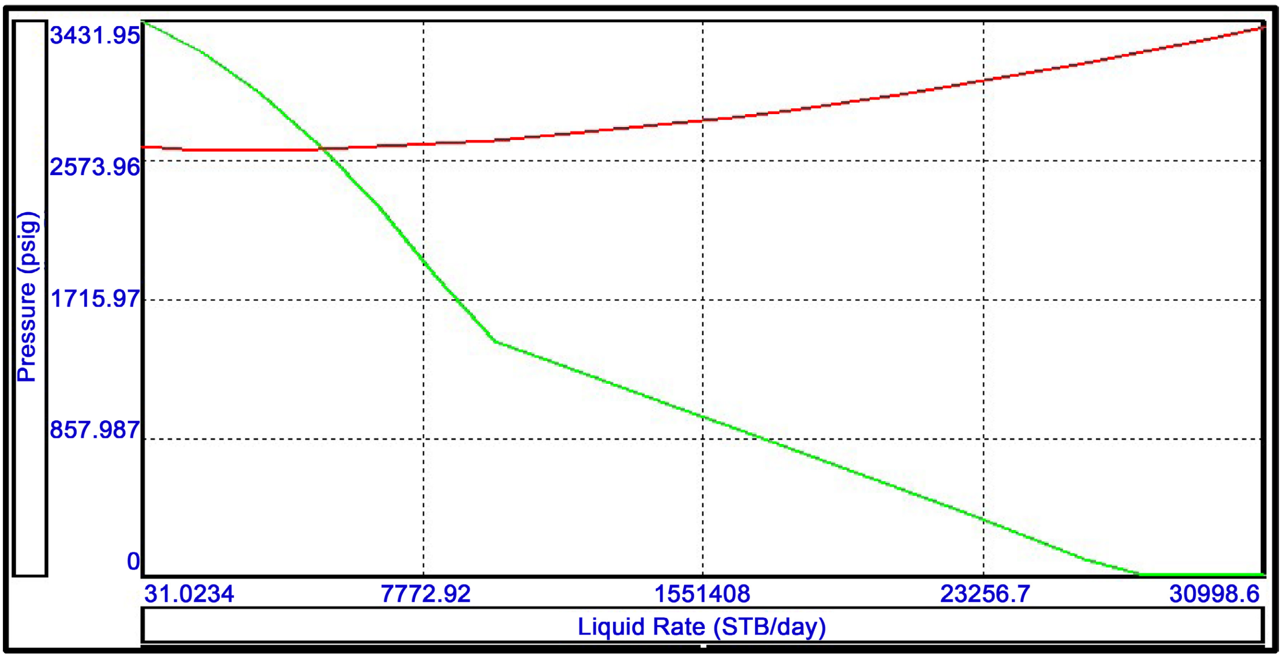

Figure 17. Plot IPR and VLP after ESP installation for well MIB-14ST2.

low STOIIP oil content and an interesting amount of water, so it would be worth reviewing the perforations at this level, or even at layer L4.

With regard to the diphasic flow in a well, the researchers were able to identify 7 flow structures that can be localized separately in the tubing. This flow regime is determined by calculating the hold up of fluid. These structures are presented as follows [27]:

- Bubble flow: this structure appears with reduced GOR values;
- Plug flow: when the GOR increases, the bubbles become wide. Combining with each other, they form gas blocks;
- Stratified flow: a large increase in GOR makes the caps long which leads to the separation of oil and gas into two stratified layers;
- Wave flow: with the increase in the volume of gas, the layered gas-oil interface becomes waves;
- Slug: by increasing the flow of gas, the GOR increases the height of the fluid waves until the peak touches the walls of the pipe;
- Annular flow: a large increase in the GOR makes the oil surrounded by the gas;
- Mist flow: at the extreme value of GOR, the liquid disperses into the gas and the flow becomes foggy.

Note: *In the case of vertical tubing, we find flow patterns such as bubble flow, stratified flow, annular flow, and slug flow.*

Knowing the negative impact of gases in the ESP pump, Figure 18 shows that the hold-up in the well is equal to 1 and the flow is in bubble flow (*i.e.* the GOR values are reduced so the presence of liquid fluids is high throughout the well.

Figure 18 shows that the hold-up in the well is equal to 1 and the flow is

Label	Bottom Measured Depth	True Vertical Depth	Pressure	Temperature	Gradient	Holdup	Regime	Heat Transfer Coefficient	Hydrates Formation	Static Gradient	Friction Gradient	Friction Pressure Loss	Gravity Pressure Loss	Slip Liquid Velocity	Slip Gas Velocity	Slip Water Velocity
	feet	*feet*	*psig*	*deg F*	*psi/ft*			*BTU/h/ft2/*		*psi/ft*	*psi/ft*	*psi*	*psi*	*ft/sec*	*ft/sec*	*ft/sec*
Liner	5821.0	5821.0	2193.17	167.00								0	0			
Liner	5739.6	5739.6	2158.73	166.99	0.42313	1.000	Bubble	8.0000		0.42283	0.0002985	0.024295	34.41	1.246	0	
Liner	5658.2	5658.2	2124.29	166.95	0.42312	1.000	Bubble	8.0000		0.42282	0.0002985	0.048592	68.83	1.246	0	
Liner	5576.8	5576.8	2089.86	166.89	0.4231	1.000	Bubble	8.0000		0.4228	0.0002985	0.07289	103.24	1.246	0	
Liner	5495.5	5495.5	2055.43	166.81	0.4231	1.000	Bubble	8.0000		0.4228	0.0002985	0.097191	137.65	1.246	0	
	5396.4	5396.4	2013.51	166.63	0.42304	1.000	Bubble	8.0000		0.42297	6.393e-5	0.10353	179.56	0.65889	0	
	5297.3	5297.3	1971.59	166.40	0.42304	1.000	Bubble	8.0000		0.42298	6.3948e-5	0.10986	221.47	0.65888	0	
	5198.2	5198.2	1929.67	166.13	0.42306	1.000	Bubble	8.0000		0.42299	6.3969e-5	0.1162	263.39	0.65886	0	
	5099.1	5099.1	1887.74	165.82	0.42307	1.000	Bubble	8.0000		0.42301	6.3994e-5	0.12254	305.30	0.65883	0	
	5000.0	5000.0	1845.82	165.46	0.4231	1.000	Bubble	8.0000		0.42303	6.4022e-5	0.12889	347.22	0.65879	0	
	5000.0	5000.0	2637.22	165.46	0.4231	1.000	ESP	8.0000		0.42303	6.4022e-5	0.12889	347.22	0.65879	0	
	4938.7	4938.7	2610.10	165.39	0.4426	1.000	Bubble	8.0000		0.42305	0.019543	1.33	373.14	6.810	0	
	4877.5	4877.5	2582.98	165.31	0.44259	1.000	Bubble	8.0000		0.42305	0.019544	2.52	399.07	6.810	0	
	4790.9	4790.9	2546.30	164.92	0.42354	1.000	Bubble	8.0000		0.42348	6.4029e-5	2.53	435.73	0.65808	0	
	4704.3	4704.3	2509.63	164.50	0.42358	1.000	Bubble	8.0000		0.42352	6.4062e-5	2.53	472.40	0.65802	0	
	4617.7	4617.7	2472.95	164.05	0.42363	1.000	Bubble	8.0000		0.42356	6.4098e-5	2.54	509.07	0.65796	0	
	4531.1	4531.1	2436.27	163.58	0.42367	1.000	Bubble	8.0000		0.42361	6.4136e-5	2.55	545.75	0.65789	0	
	4444.5	4444.5	2399.58	163.08	0.42372	1.000	Bubble	8.0000		0.42366	6.4176e-5	2.55	582.43	0.65781	0	
	4358.0	4358.0	2362.89	162.55	0.42377	1.000	Bubble	8.0000		0.42371	6.4218e-5	2.56	619.12	0.65773	0	
	4258.9	4258.9	2320.47	162.29	0.42826	1.000	Bubble	8.0000		0.42338	0.0048809	3.04	661.05	3.889	0	
	4159.9	4159.9	2278.05	162.01	0.42827	1.000	Bubble	8.0000		0.42339	0.0048821	3.52	702.99	3.889	0	
	4060.8	4060.8	2235.63	161.71	0.42829	1.000	Bubble	8.0000		0.42341	0.0048833	4.01	744.92	3.889	0	
	3961.8	3961.8	2193.21	161.39	0.42831	1.000	Bubble	8.0000		0.42343	0.0048847	4.49	786.86	3.889	0	
	3862.7	3862.7	2150.79	161.06	0.42834	1.000	Bubble	8.0000		0.42345	0.0048861	4.98	828.80	3.889	0	

Figure 18. Hold-up evolution at depth in the MIB-14ST2 well.

bubble flow, *i.e.* GOR values are reduced, so the presence of liquid fluids is high throughout the well.

As the water requirement for the pump is very high, this does not adversely affect pump performance, whereas the viscosity of fluids in the well is considered a variable that can affect well performance. This significantly reduces pump performance in the case of viscous or overly viscous fluids. When fluid viscosity is high, the number of rotating parts (rotor) is high and creates a lot of friction surfaces, which results in high energy losses in the well. In the case of the well under study, we'll try the sensitivities of frequency and number of pump stages, as the oil in the upper Pinda reservoir has a good viscosity of 1.1 Cp.

Once the liquid level has been obtained in TVD, we need to relate it to the depth measurement and according to the well deviation in order to measure the tubing fill volume [21]. This gives:

$$t_{SURF} = \frac{V_{TUBING}}{Q_{PUMP}} \tag{17}$$

With:

- t_{SURF}: pumping time, minute or second;
- V_{TUBING}: tubing volume, cubic meter;
- Q_{PUMP}: estimated fluid flow pump output, stb.

To calculate the tubing volume of an oil well, you need to take into account the dimensions of the tubing, *i.e.* its inside diameter and length (**Table 4**). Tubing volume an oil well can be calculated using the volume of the cylindrical tubing:

$$V_{tubing} = \frac{\pi * ID^2 * l_t}{4} \quad \text{in cubic feet} \tag{18}$$

With:

- l_t: tubing length, feet;

- *ID*: Inside diameter, inch.

Equation (17) and Equation (18) were used to calculate the pumping time. For the MIB-14ST2 well, the tubing volume is 232.19 ft3 and the surface fluid pumping time is 11 minutes and 9 seconds.

4. Discussions

During production using Gas-lift activation, the well was producing 70 barrels of oil per day (BOPD) with a water-oil ratio (WOR) of 68%. After converting to ESP activation, the well is expected to produce 75 BOPD with a water flow rate of 4926.6 barrels of water per day (BWPD). It is observed that the increase in oil production is only 5 BOPD, but with a WOR of 98% and a low gas flow rate. The low gas production is an indicator that the Gas-lift activation mode was inadequate for this well, while the presence of water provides a strong argument for activating the well in ESP mode. Unfortunately, instead of producing a higher oil flow rate, the well is producing more water.

However, the pump depth is set at 5000 ft, and after simulation, the pump head is at 1877.38 ft. Therefore, this excessive water production indicates that either the water column in the well has reached the perforation zones, the layers traversed by the well are water-bearing rather than oil-bearing, or there is the presence of an aquifer in the vicinity of the perforated zones.

Analyzing **Figure 5**, we observe that the perforation depths are located between 5346 to 5376 ft MDRT, 5532 to 5616 ft MDRT, 5626 to 5670 ft MDRT, 5735 to 5755 ft MDRT, and 5757 to 5777 ft MDRT, and do not negatively impact the pump position. Additionally, out of the seven layers subdividing the upper Pinda reservoir according to **Table 1** and **Table 2**, this well under study traverses four layers, namely:

- L1 is a limestone layer with 17% porosity and 5 mD permeability, containing 132.3 million stock tank barrels (MMstb) of oil reserves;
- L2 is a dolomite layer with 10% porosity and 15 mD permeability, containing 86.9 MMstb of oil reserves;
- L4 is a sandstone layer with 10% porosity and 37 mD permeability, containing 99 MMstb of oil reserves;
- L5 is another sandstone layer with 10% porosity and 49 mD permeability, containing 7.7 MMstb of oil reserves.

Unfortunately, the studies conducted in 2016 did not quantify the water reserves in the reservoir and did not identify the presence of an aquifer in the vicinity of the reservoir. It is noted that the well traverses 325.9 million stock tank barrels (MMstb) of oil reserves contained in the diverse lithological nature (limestone, dolomite, and sandstone) of the upper Pinda reservoir.

Although all conditions seem to be met for the well to be activated in ESP mode, after a thorough analysis of the data and results obtained during the evaluation and optimization of the production system of the Mibale field from MIB-14ST2 well, it is evident that converting the activation mode is not the optimal solution to improve oil production in this field. Therefore, other factors may contribute to the decline in oil production in the Mibale field, including:

- Reservoir pressure decline necessitating an enhanced recovery method;
- Petrophysical characteristics of the reservoir;
- Oil flow obstruction due to sediment accumulation, particles, or other substances in the reservoir pores (porosity plugging);
- Aging or damage to production equipment (technical issues, equipment failures, or delays in equipment replacement such as pumps or valves);
- Insufficient bottom-hole pressure limiting fluid flow to the surface.

After reviewing various reports from the operating company, it appears that workover studies were conducted in 2010 to replace old equipment and clean well MIB-14ST2 with the aim of improving well productivity. Therefore, considering the factors mentioned earlier, the issue of equipment aging can be excluded. Additionally, one of the objectives of converting the activation mode to ESP is to more effectively control bottom-hole pressure. Hence, the problem of insufficient bottom-hole pressure in well MIB-14ST2 is completely resolved by the activation mode conversion.

Given the limitations of nodal analysis techniques in detecting all potential issues in a production system, results are often combined with reservoir simulations to enhance precision regarding the performance of the production system. This integration can lead to more informed decisions when optimizing production. Consequently, the unsatisfactory results obtained from this study have prompted the proposal of additional complementary studies on reservoir behavior and quantification of remaining reserves in the present day to assist the upper Pinda reservoir. The reservoir simulation will address the limitations of nodal analysis in the following ways:

- Detailed Reservoir Modeling: Reservoir simulations will provide a better understanding of the interaction between the wells and the reservoir, taking into account the complex geometry of the reservoir, heterogeneities, aquifer barriers, etc.;
- Reservoir simulation models will integrate mass and energy conservation equations to simulate multiphase flows, interactions between gas and liquid, capillary effects, etc., providing a more comprehensive view of production processes;
- Production Scheme Optimization: Reservoir simulations will offer a more in-depth approach to various production strategies, injection schemes, optimal production rates, etc., to maximize the oil field's yield.

Therefore, it is essential to complement this study with reservoir simulations to identify the true factor contributing to the low production in the Mibale field.

5. Conclusion and Perspective

Nowadays, investment in the oil sector has become scarce due to the energy transition decided by funders. However, oil and gas still remain the only energy consumed in various forms worldwide, accounting for more than 60% of the total. Therefore, to avoid an energy crisis during this transition period, it is necessary to maximize the extraction of already discovered reserves, such as the mature fields being exploited in the Kongo central province, in the Democratic Republic of the Congo.

These already discovered reserves face various issues, including declining reservoir pressure, aging well equipment, inappropriate well activation methods, or inefficient reservoir recovery methods. Therefore, our study aimed to evaluate and optimize the production system of the Mibale field, specifically focusing on the MIB-14ST2 well located offshore in the coastal basin of the Democratic Republic of the Congo. Our main objective was to enhance the performance, efficiency, and sustainability of the hydrocarbon production system in the Mibale field by proposing appropriate well activation methods for the MIB-14ST2 well, which is considered the least productive well in the field with an average flow rate of 70 stb/day.

After collecting and analyzing geological, reservoir, and production data using appropriate tools and techniques such as Excel and IPM Prosper simulation software for production system modeling, we evaluated well MIB-14ST2 based on three key elements. The first element was the IPR to assess the production capacity of the well in relation to the reservoir, the second element was the VLP to identify the well performance (including tubing pressure losses), and the third element focused on dynamic production parameters such as water cut, GOR, first node pressure, etc., to better understand the production dynamics of the well and optimize overall performance. This evaluation aimed to determine whether it was advantageous to optimize the production of the well.

Plotting the IPR and VLP graphs, we observed that well MIB-14ST2 had the capacity to produce a total liquid flow rate of 30998.8 stb/day, consisting of 464.978 bbl/day of oil and 30533.822 stb/day of water. Based on this production capacity of the well, it was evident that the well could still yield a significant amount of oil. Thus, the proposal to convert the Gas-lift activation mode to ESP was put forward for this well. By utilizing simulations of the well using IPM Prosper software, we obtained the parameter values or necessary conditions for MIB-14ST2 well to produce with this new activation mode.

Subsequently, at a depth of 5000 ft and a pump head of 1877.38 ft, the pump must be installed and should consist of 76 stages operating at a frequency of 50 Hertz, resulting in the well producing 75 stb/day of oil, 0.022 MMscf/day of gas, and 4926 stb/day of water. It is important to note that several scenarios were explored by varying the pump type, frequencies, and other variables in an attempt to achieve a higher oil production rate from this well. Unfortunately, the observation remains that the well continues to produce a very low oil flow rate.

As a result, it is evident that several factors may be influencing the excessive water production compared to oil in this well, including perforation depths, the layers traversed by the well, water infiltration from an unidentified aquifer, etc.

Identifying the factors influencing this low oil production is complex due to the fact that oil wells are part of a complex system that includes the reservoir and collection networks (surface equipment, pipelines, valves, etc.). It is worth noting that nodal analysis does not fully consider the interactions between these components, which could limit its effectiveness in optimizing MIB-14ST2 well. Based on the results obtained from this nodal analysis, which is a part of our work in this field, we are considering further studies on the simulation of the upper Pinda reservoir to understand the variations in petrophysical parameters and estimate the remaining oil reserves.

This approach will allow us to resume water injection, which was halted in 2010 in this field due to the inefficiency of the process. This could lead to a significant improvement in the production of the Mibale field and the management of the well production system. As the upper Pinda reservoir is multilayered, in order to decide on the layer to inject water into, it would be advisable to simulate all seven layers comprising this reservoir while taking into account their petrophysical characteristics and fluid contents.

This will require further study on revising the surface facilities for injection water treatment and also potentially converting some producers into injectors or drilling new wells.

Acknowledgements

We would like to thank Perenco Rep-MIOC for making its production reports and data available to us, and its engineers from the Geosciences and Production Department for fruitful exchanges with a view to finding lasting solutions for improving production from its onshore and offshore fields.

Conflicts of Interest

The authors declare no conflicts of interest regarding the publication of this paper.

References

[1] Aarts E.H.L. and Lenstra J.K. (2003) Local Search in Combinatorial Optimization: Algorithms, Geometry and Applications, Stochastic Operations Research and Combinatorial Optimization. Wiley-Interscience, Hoboken. https://doi.org/10.1515/9780691187563

[2] Corne D., Dorigo, M. and Glover, F. (1999) New Ideas in Optimization. McGraw-Hill Ltd., New York.

[3] (2023) https://www.oil-gasportal.com/petroleum-production-optimization/

[4] Faires, J.D. and Burden, R.L. (2004) Numerical Analysis. 8th Edition, Cengage Learning, Boston.

[5] Ahmed, T. (2001) Reservoir Engineering Handbook. 2nd Edition, Gulf Professional Publishing, Houston.

[6] Satter, A. and Iqbal, G.M. (2015) Reservoir Engineering: The Fundamentals, Simulation, and Management of Conventional and Unconventional Recoveries. Elsevier

Gulf Professional Publishing, Houston.

[7] Guo, B.Y., Lyons, W.C. and Ghalambor, A. (2007) Petroleum Production Engineering: A Computer-Assisted Approach. Elsevier Science & Technology, New York. https://doi.org/10.1016/B978-075068270-1/50005-0

[8] Abdoulaye, W., Capo, P., George, P. and James, B. (2007) Mibale Field Reservoir Simulation Study. PERENCO MIOC, Geosciences and Production Offices, Moanda, p. 89.

[9] Ejike, C. (2021) Gas Injection Transport Mechanism for Shale Oil Recovery. *International Journal of Energy and Environmental Engineering*, **15**, 288-292.

[10] Jansen, J.D. (2017) Nodal Analysis of Oil and Gas Production Systems. Society of Petroleum Engineers, Houston. https://doi.org/10.2118/9781613995648

[11] Simonnard, M. (1962) Linear Programming. Dunod, Paris.

[12] Allen, J., Béhéret, A., Lepvaraud, A., Labudovic, M., Josseron, E. and Fabre, N. (2016) Mibale Upper Pinda Evaluation Offshore DRC. PERENCO MIOC, Geosciences and Production Offices, Moanda, p. 61.

[13] Capo, P. (2010) Mibale Development—Water Injectors Work over Proposal. PERENCO MIOC, Geosciences and Production Offices, Moanda, p. 29.

[14] Jean, O.N., Bruno, D.O., Dominique, W.O., Patrick, L.E., Richard, K.L., Cedrick, K.M., Djonive, M.A. and Shams, M.D. (2021) Assessment of Aquifer Performance for Oil Drainage in the Upper Pinda Reservoir of the Mibale Field. *Petroleum Science and Engineering*, **5**, 13-31. https://doi.org/10.11648/j.pse.20210501.12

[15] Thimaiah, P. (2005) Introduction to Hydrocarbon Exploitation, Well Testing. Albat Solution Limited.

[16] Glaso, O. (1980) Generalised Pressure Volume Temperature Correlations. *Journal of Petroleum Technology*, **32**, 785-795. https://doi.org/10.2118/8016-PA

[17] Gay, L. (1982) Activation of Wells by Electric Centrifugal Pumping. DPRO-EXPLO-PUITS.

[18] (2014) Petroleum Experts, Prosper User Manual, Single Well Systems Analysis, Version 13.0. https://fr.scribd.com/document/299781735/PROSPER-Complete

[19] Mohammed, M.D. (2014) Proposed Correlation for Gas Solubility at and below Bubble Point Pressure. *Engineering and Technology Journal*, **32**, 1497-1505. https://doi.org/10.30684/etj.32.6A.12

[20] Vogel, J.V. (1968) Inflow Performance Relationship for Solution-Gas Drive Wells. *Journal of Petroleum Technology*, **20**, 83-92. https://doi.org/10.2118/1476-PA

[21] Cholet, H. (2000) Well Production Pratical Handbook. Editions Technips, Paris.

[22] Brown, K.E. (1977) The Technology of Artificial Lift Methods. Pennwell Books, Tulsa.

[23] Dale, B.H. (2003) Production Optimization Using Nodal Analysis. 2nd Edition, OGCI and Petroskills Publications, Tulsa.

[24] Benzerga, A. and Aroudji, M. (2016) Artificial Lift Using a Submersible Electric Pump, Case Study: AMA #52 - AMA #09 Wells, Application in the TFT Field. https://dspace.univ-ouargla.dz/jspui/bitstream/123456789/13026/1/Lifting_Artificiel_Par_Une_Pompe_electrique_Immergee.pdf

[25] Arutunoff, A. (1936) Inventing the Electric Submersible Pump American Oil & Gas Historical Society. Petroleum Technology, Stavanger, p. 81.

[26] Jansen, J.D. and Currie, P.K. (2004) Modelling and Optimisation of Oil and Gas

Production Systems. Edition Section Petroleum Engineering, Texas.

[27] Takacs, G. (2009) Electrical Submersible Pump Manual: Design, Operations, and Maintenance. Elsevier, New York.

Abbreviations

B_o: oil volumetric factor in bbl/stb
F_t: the friction in the tubing expressed in height
H_d: height or vertical distance (in ft) from wellhead to estimated production fluid level at design capacity
P_d: the friction in the surface pipe expressed in height
P_r: reservoir pressure in psi
P_{wf}: downhole flow pressure in psi
Q_o or q_o: oil flow rate, stb/day
R_s: Ratio of gas dissolved in oil
V_m: Mixture surface speed
r_e: drainage radius in feet
r_w: wellbore radius in feet
μ_o: oil viscosity in centipoise
d: diameter of tubing, in
ft: feet
h: pump head in ft
hp: horsepower
VLP: Vertical Lift Performance
k: permeability in mD